Research Article Vol. 4, No. 3 / March 2017 / Optica 334

Impact of internal curvature gradient on the power and accommodation of the crystalline lens

Rafael Navarro[1] and Norberto López-Gil[2,*]

[1]Consejo Superior de Investigaciones Científicas & Universidad de Zaragoza, ICMA, P. Cerbuna, 12, Zaragoza 50009, Spain
[2]Universidad de Murcia, Instituto Universitario de Investigación en Envejecimiento, Murcia 30100, Spain
*Corresponding author: norberto@um.es

Received 15 July 2016; revised 30 January 2017; accepted 3 February 2017 (Doc. ID 270373); published 6 March 2017

Human crystalline lens has a layered, shell-like structure with the refractive index increasing from cortex to nucleus (gradient index or GRIN structure). Moreover, every iso-indicial layer has a certain curvature which also varies from cortex to nucleus, with a gradient of curvature (G). In the present manuscript, the role of G on the lens power is investigated along with its implications regarding the lens paradox (change of lens power with age) and intra-capsular accommodation mechanism (larger than expected changes of lens power during accommodation compared to a homogenous lens). To this end, a simplified formulation of paraxial lens power based on thin lens approximation is developed and applied to the anterior and posterior parts of the lens. The main theoretical result is that the power of both anterior and posterior lens is given by the sum of the power of a lens with a homogeneous refractive index equal to that of the nucleus and power associated with the contribution of the internal GRIN structure, which depends on G. This general result suggests that the sign of G is fundamental in increasing or decreasing the lens power. We found that the curvature gradient has a strong impact on lens power, helping to explain both the lens paradox and intra-capsular accommodation mechanism.

OCIS codes: (140.3490) Lasers, distributed-feedback; (060.2420) Fibers, polarization-maintaining; (060.3735) Fiber Bragg gratings; (060.2370) Fiber optics sensors.

https://doi.org/10.1364/OPTICA.4.000334

1. INTRODUCTION

The human crystalline lens has a complex GRIN internal structure and shows substantial changes both with age and accommodation [1]. The power of young lenses can increase by 50% or even more during accommodation, whereas the lens tends to lose power with age [2]. An important open question is how much of these changes are due to its GRIN structure.

Important efforts were dedicated to measure both its structure [3–6] and optical performance [7,8], and a number of models [9–12] were developed trying to link structure to function. Despite all these efforts, the optics of the human lens—as well as its changes with age and accommodation—are not totally understood yet. For instance, the Brown's lens paradox [13] refers to the fact that the curvature of lens surfaces increases with age and yet the lens loses refracting power. Several explanations for this paradox have been proposed [14–18], but it is probably a symptom of important unknowns which cause the lens models to fail to accurately predict the changes associated with age and accommodation.

There is a wide variety of lens models of increasing complexity, from the simplest homogeneous lens model [19] to the four-surface or two-compartment (cortex and nucleus) models [20] and the more realistic GRIN models. Nevertheless, even the more sophisticated models [10,11] are based on simplifying assumptions, which might be unrealistic. One particularly common simplification is assuming that the iso-indicial surfaces of the GRIN structure are concentric. This means that the apical (axial) curvature radius r decreases linearly with the axial depth z, that is, $r^{\text{ant}}(z) = R_s^{\text{ant}} - z$ and $r^{\text{pos}}(z) = R_s^{\text{pos}} + t - z$ for the anterior and posterior parts of the lens, respectively. Here, R_s^{ant} and R_s^{pos} are the radii of the anterior and posterior external (lens surface) iso-indicial surfaces, respectively, and t is the thickness of the lens. Thus, when the iso-indicial surfaces are concentric, their curvature radii have a negative gradient of −1. On the contrary, as curvature is the inverse of the radius, the iso-indicial curvature will have a positive gradient. However, experimental studies suggest that iso-indicial surfaces are not always concentric, and the inner curvature gradient may differ among individuals and probably is higher for young lenses [4,21]. In other words, the simplifying assumption of concentric iso-indicial surfaces does not seem to be realistic, and the gradient of the curvature radius may take other values different from −1. Indeed, a recent lens (AVOCADO) model [22] was proposed which is more general in the sense that it considers two independent axial and radial GRIN distributions, and hence the iso-indicial surfaces are not necessarily concentric. These two independent distributions allow for the decoupling of its refractive power and axial optical path length.

Our goal in this work is to study the role of the curvature gradient on the power and amplitude of accommodation of the lens. The main assumption applied here is conceptually different from the AVOCADO model [22] since we do not consider two independent axial and radial distributions, but instead we consider two independent gradients along the axial (z) direction: refractive index and curvature. This means a relatively simple and direct generalization of the concentric GRIN distribution, which will permit us to study the role of the inner curvature gradient on the power and amplitude of accommodation of the lens.

2. METHODS

In what follows, we study the influence of the GRIN on the total power of the lens. To this end, we develop a theoretical and numerical analysis of the combined role of the gradients of refractive index and curvature along the z (axial) direction. As usual, we divide the lens into anterior and posterior parts. Then we will focus the theoretical analysis on the anterior part since the analysis of the posterior part is equivalent. For simplicity, here we apply the paraxial approximation (Gaussian optics) to compute the lens power. Therefore, we do not need to consider the radial distribution of refractive index and we assume that both refractive index and inner curvature only depend on the axial coordinate z.

We assume an expression for the curvature gradient:

$$r(z) = R_s - Gz, \qquad C(z) = \frac{1}{R_s - Gz}. \tag{1}$$

Note that all parameters and variables should have the superscript ant as they correspond to the anterior part of the lens: r^{ant}, R_s^{ant}, G^{ant}, etc. For the sake of clarity, the superscripts are omitted in all the equations unless they are necessary to distinguish between anterior and posterior. For the distributions of Eq. (1), the gradient of radius is $dr/dz = -G$, whereas the curvature gradient is $dC/dz = G/r^2$. We will call G the curvature gradient parameter. When $G = 0$, the curvature is constant and the iso-indicial surfaces are parallel; for $G = 1$, the iso-indicial surfaces are concentric. The concentric distribution is important because it has been used in most GRIN lens models. Equation (1) is more general since it includes the concentric distribution as a particular case, but it also allows us to study other GRIN distributions where G may have other positive or negative values. Figure 1 shows several examples of iso-indicial surfaces of the anterior lens for different G values.

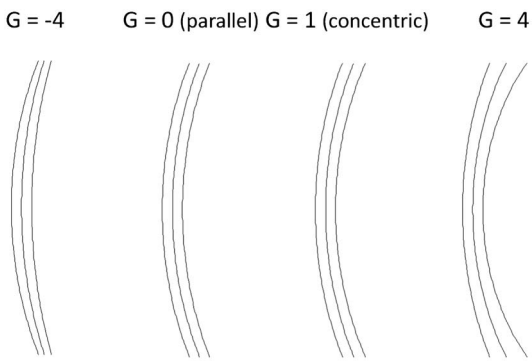

Fig. 1. Examples of iso-indicial contours for different values of the curvature gradient parameter G.

A. Theoretical Analysis

For the computation of the paraxial power, we apply the thin lens approximation, applied to both the anterior and posterior parts of the lens, and then we combine anterior and posterior powers using the thick lens approximation:

$$P^{\text{lens}} = P^{\text{ant}} + P^{\text{pos}} - e_{\text{effective}} P^{\text{ant}} P^{\text{pos}}, \tag{2}$$

where $e_{\text{effective}} = \frac{t_{\text{effective}}}{n_{\text{effective}}} \approx \frac{t}{n_n}$.

Here, n_n is the refractive index at the nucleus center. This provides a strong simplification. The effectiveness of this approximation will be validated *a posteriori* by comparing the theoretical results with paraxial ray tracing performed using Zemax (ZEMAX, LLC, Kirkland, WA USA).

Under the thin lens approximation, the power of the anterior part (equivalent to the posterior) is given by the sum of all contributions. Here we consider shell and continuous lens models. The power of the finite shell model is given by

$$P = (n_s - n_0)C_s + \sum_{i=1}^{N}(n_{i+1} - n_i)C_i = \sum_{i=0}^{N}(n_{i+1} - n_i)C_i, \tag{3a}$$

where N is the number of shells of the anterior (or posterior) part and, for the continuous model,

$$P = (n_s - n_0)C_s + \int_0^{t_{\text{ant}}} \frac{dn(z)}{dz} C(z)\mathrm{d}z, \tag{3b}$$

where t_{ant} is the axial thickness of the anterior part of the lens, C_s is the curvature of the external surface, and C_i (surface of the ith shell in the discrete model) or $C(z > 0)$ (continuous model) are the internal curvatures. For simplicity, we assume $C_0 = C_s$ or $C(z = 0) = C_s$. Similarly, $n_0 = n(z < 0)$ is the refractive index of the surrounding medium (aqueous humor); $n_1 = n(z = 0) = n_s$ is the refractive index of the external surface of the lens; and $n(z = t_{\text{ant}}) = n_{N+1} = n_n$. Both the surface [first term in Eq. (3)] and the inner structure (second term) contribute to the lens power.

Now, we can analyze the simplest case of $G = 0$, which is constant curvature, i.e., parallel iso-indicial surfaces. For the shell model [Eq. (3a)], $C_i = C_s.C_i$ is a common factor that we can extract from the sum, so that $P = C_s \sum_{i=0}^{N}(n_{i+1} - n_i)$. Then all intermediate values n_i cancel each other except for the two extreme values:

$$(n_1 - n_0) + (n_2 - n_1) + (n_3 - n_2) + \ldots + (n_{N+1} - n_N) = n_{N+1} - n_0 = n_n - n_0.$$

Therefore, the power for the discrete shell model for the case $G = 0$ is

$$P = (n_n - n_0)C_s = P_{\text{HOM}}, \tag{4}$$

where P_{HOM} is the power of a (single-surface) lens with a homogeneous refractive index corresponding to that of the nucleus. The same result is obtained for the continuous model of Eq. (3b). $C(z) = C_s$ and we can take it out from the integral. Now the integral is trivial: $n(z)]_0^{t_{\text{ant}}} = n_n - n_s$. Thus it easy to show that, for $G = 0$, Eq. (3b) reduces to Eq. (4). Note that a totally equivalent result is obtained for the posterior part ($P^{\text{pos}} = (n_0 - n_n)C_s^{\text{post}}$, with $C_s^{\text{pos}} < 0$). Thus, we can introduce the values $P^{\text{ant}} = P_{\text{HOM}}^{\text{ant}}$ and $P^{\text{pos}} = P_{\text{HOM}}^{\text{pos}}$ in Eq. (2) so that, in absence of curvature gradient ($G = 0$), the power of the lens is

equal to that of a lens with a homogeneous refractive index equal to its central value n_n. The most interesting aspect of this result is that it is totally general, independent from the type (discrete or continuous) of axial distribution of refractive index $n(z)$.

When $G \neq 0$, the analysis is not as simple because in Eq. (1) we assumed that the curvature is a nonlinear function of z. Nevertheless, we can apply a Taylor series expansion to obtain a polynomial approximation:

$$C = \frac{1}{R_s - Gz} = \frac{C_s}{1 - C_s G z} \approx C_s + GC_s^2 z + G^2 C_s^3 z^2 + \ldots = C_s + Gf(z), \tag{5}$$

with $f(z) = C_s^2 z + GC_s^3 z^2 + \ldots$. The resulting expression for C is now similar to that of the radius in Eq. (1), but now we have the polynomial $f(z)$ instead of z. Notice that the curvature is defined only inside the lens. Thus, z is always positive ($0 < z \leq t$). It is easy to realize that, for typical values of curvatures and axial thicknesses in human lenses, $f(z)$ is always positive.

We can substitute the polynomial expansion of C in Eq. (5) in Eq. (3b):

$$P = (n_s - n_0)C_s + \int_0^{t_{\text{ant}}} dn/dz(C_s + Gf(z))\mathrm{d}z = (n_n - n_0)C_s + G\int_0^{t_{\text{ant}}} dn/dz f(z)\mathrm{d}z. \tag{6a}$$

This can be rewritten as

$$P = P_{\text{HOM}} + P_{\text{GRIN}} = P_{\text{HOM}} + Gp_{\text{GRIN}}, \tag{6b}$$

with

$$p_{\text{GRIN}} = \int_0^{t_{\text{ant}}} dn/dz f(z)\mathrm{d}z. \tag{6c}$$

This is a general expression (equivalent result applies to the posterior part), which means that the power of the anterior part of the lens has two contributions. The first contribution $P_{\text{HOM}} = (n_n - n_0)C_s$ is constant and totally independent of the type of refractive index gradient or curvature gradient parameter G. The second term, $P_{\text{GRIN}} = Gp_{\text{GRIN}}$, is the product of G with the integral of Eq. (6c): G represents the specific contribution of the curvature gradient whereas p_{GRIN} represents the specific contribution of the refractive index gradient. For the shell model, we only have to change the integral by the finite sum to obtain an equivalent expression. This is a general and important result, which means that both curvature G and refractive index dn/dz gradients conjointly enhance the power of the lens. Equations (6a) and (6b) are not totally exact since they rely on the thin lens approximation (TLA), which assumes that the cross term $-e_{\text{effective}}P^{\text{ant}}P^{\text{pos}}$ in Eq. (2) can be neglected. We can use the simple four-surface shell model to estimate the validity of the TLA. To this end, we treat this shell model as the coupling of two (anterior and posterior) lenses. Thus, we apply Eq. (2) three times: one for the anterior lens, another for the posterior lens, and finally to the coupling of both parts. Note that when applied to the anterior lens, P^{ant} means the power of the anterior surface of the cortex and P^{pos} is the power of the anterior surface of the nucleus (and analogous to the posterior lens). The resulting values are $P^{\text{ant}} = 7.30\text{D}$ and $P^{\text{pos}} = 15.42\text{D}$. If we neglect the cross term (TLA), then we have $P^{\text{ant}}_{\text{TLA}} = 7.31\text{D}$ and $P^{\text{pos}}_{\text{TLA}} = 15.44\text{D}$. This means that the error associated with the TLA is below 0.15%. The reason for this is that the thickness of the cortex is 0.55 mm, meaning that in fact the lens cortex is a thin lens. However, for the coupling of both parts of the lens, we have that the total power of the lens is $P^{\text{lens}} = 22.45\text{D}$ but $P^{\text{lens}}_{\text{TLA}} = 22.75\text{D}$—a difference of 0.3 D (1.3%), which is clinically relevant. This percentage can be somewhat larger in the accommodated lens. Therefore, we conclude that the TLA is valid for the lens cortex (anterior and posterior parts), but not to compute the total power of the lens (coupling of the anterior and posterior parts). For this purpose, we can combine Eqs. (2) and (6b), and operate to obtain the expression of the total power of the lens:

$$P^{\text{lens}} = P^{\text{lens}}_{\text{HOM}} + P^{\text{lens}}_{\text{GRIN}} - \frac{t}{n_n}\left(P^{\text{ant}}_{\text{HOM}} * P^{\text{pos}}_{\text{GRIN}} + P^{\text{pos}}_{\text{HOM}} * P^{\text{ant}}_{\text{GRIN}}\right). \tag{7}$$

Equation (7) contains cross terms that cannot be ignored. In subsequent sections, we will see that this combined use of thin lens (for anterior and posterior parts) and thick lens (for the whole lens) approximations provides values close enough to those obtained by ray tracing.

B. Application to a GRIN Model

The integral of Eq. (5) can be solved knowing the distribution of the refractive index along the axis $n(z)$, which depends on the particular model used. As an example, here we assume the axial distribution of a previous model [23] consisting of a continuous concentric gradient distribution ($G = 1$), which follows a classical power law. For the anterior and posterior parts of the lens, this is given by

$$n^{\text{ant}}(z) = n_n - (n_n - n_s)(1 - \xi^{\text{ant}})^p, \tag{8a}$$

with $\xi^{\text{ant}} = \dfrac{z^2 - 2zR_s^{\text{ant}}}{t_{\text{ant}}^2 - 2t_{\text{ant}}R_s^{\text{ant}}}$, and

$$n^{\text{pos}}(z) = n_n - (n_n - n_s)(\xi^{\text{pos}})^p, \tag{8b}$$

with $\xi^{\text{pos}} = \dfrac{(z - t_{\text{ant}})^2 - 2(z - t_{\text{ant}})(R_s^{\text{pos}} - t_{\text{pos}})}{t_{\text{pos}}^2 - 2t_{\text{pos}}(R_s^{\text{pos}} - t_{\text{pos}})}$.

Here, p is an age-dependent exponent; t_{pos} and R_s^{pos} are the thickness and surface radius of the posterior part of the lens, respectively. Both ξ^{ant} and ξ^{pos} take values within the interval [0,1]. The parameters of this model change with age and accommodation, as explained in Ref. [19]. In what follows, we considered the case of a 20-year-old lens for both far and near (accommodated) viewing. Three different types of model were implemented using the same geometrical and refractive index parameters: (a) homogenous lens with refractive index n_n; (b) four-surface shell model; and (c) GRIN model after Eq. (8). The paraxial power of these models is computed in two ways: (1) through numerical implementation of the just-discussed equations as a MATLAB code (MathWorks, Natick, Massachusetts, USA); and (2) paraxial ray tracing implemented in Zemax. The later will be used for validating the approximations assumed in our theoretical analysis.

3. RESULTS

In this section, we analyze both theoretical and numerical results of the impact of the curvature gradient parameter G on the power and amplitude of accommodation of the lens.

A. Theoretical Predictions

The main theoretical result was presented previously, and is summarized by Eq. (6b): $P = P_{\mathrm{HOM}} + P_{\mathrm{GRIN}}$ with $P_{\mathrm{GRIN}} = Gp_{\mathrm{GRIN}}$. This means that the power of either the anterior or posterior part of the lens is the sum of the power of a (single-surface) lens with homogeneous refractive index n_n and the power generated by the GRIN internal structure. For the complete lens, we have to apply Eq. (7), and hence the total power of the lens is not a simple sum of the different contributions. The interesting particular case of $G = 0$, $P = P_{\mathrm{HOM}}$ tell us that when there is no curvature gradient and the iso-indicial surfaces are parallel, then the power of the lens is equal to the power of a lens with homogeneous refractive index n_n. A second and most interesting possibility is when $G > 0$. In this case, there is an additional positive contribution of the GRIN internal structure which will produce an enhancement of lens power. The higher the value of G, the higher the power of the lens. In addition, $f(z)$ contains higher-order terms with powers of G (and is positive when $G > 0$); thus, we should expect that the increase of power may show some acceleration as G increases. In the third and last case $G < 0$, the term Gp_{GRIN} will be negative and the lens power will not be enhanced but decreased with respect to the power of a homogeneous lens. These predictions are further analyzed with the numerical examples in the next section.

B. Numerical Results

Here we present results obtained for three lens models, homogeneous, four-surface, and GRIN, all of which are based on the GRIN model [23]. All surfaces will be considered spherical and the axial thickness of the cortex (both anterior and posterior) will be 0.5 mm, which is not far from experimental values [24]. Thus, the thickness of the nucleus was obtained by subtracting 1 mm from the total lens thickness. We are interested in studying the effect of G on the paraxial power of the lens, its equivalent refractive index, and the power increment with accommodation.

1. Homogeneous and Shell Lenses

The first and more important cross-validation was carried out using the homogeneous and four-surface shell model, which allows the G parameter to be scanned easily. Figure 2 shows a close agreement between the lens power obtained by paraxial ray tracing using Zemax (blue line and circles) and that obtained by theoretical calculations (red line and stars), using Eq. (3a) based on TLA. The agreement is good independent of the value of G, which confirms the validity of the TLA. In addition we confirm the theoretical prediction that, for $G = 0$, the lens power is the same as that of a homogeneous lens. As predicted, another important result is that we can observe an accelerated (nonlinear) increase of the lens power with G. Conversely, for $G < 0$, the power is lower than that of the homogeneous lens.

2. GRIN Lens

Figure 3 is similar to Fig. 2, but for the continuous GRIN distribution [Eq. (3b)]. The GRIN model implemented in Zemax for finite and paraxial ray tracing is concentric so it corresponds to the case of $G = 1$. Thus, the Zemax (GRIN model) is plotted as a single brown dot. The paraxial power of the homogeneous lens (red asterisk) is also included for reference. The agreement between the theoretical and ray-tracing results is reasonable in both cases. As an example of the impact of the gradient of curvature, if we consider the power of the homogeneous lens ($G = 0$) of 21.34 D, a gradient of $G = 3$ increases the lens power up to 24.12 D, that is, nearly 3 D (13%).

The equivalent refractive index n_{eq}, usually defined as the refractive index of a homogeneous lens having the same external geometry and same power as the GRIN lens [20,25], is shown in Fig. 4. As one might expect, both paraxial power and equivalent refractive index show a similar trend with G.

For $G = 0$, $n_{\mathrm{eq}}(G = 0) = n_n$ (1.418 in our model), whereas n_{eq} increases or decreases depending on the sign of G. Interestingly, the range of values contained in this plot is consistent with experimental data despite the important differences found among different studies [25].

3. Accommodation

The impact of G on the amplitude of accommodation is illustrated in Fig. 5. The paraxial power increase was computed as the difference between the power of the unaccommodated

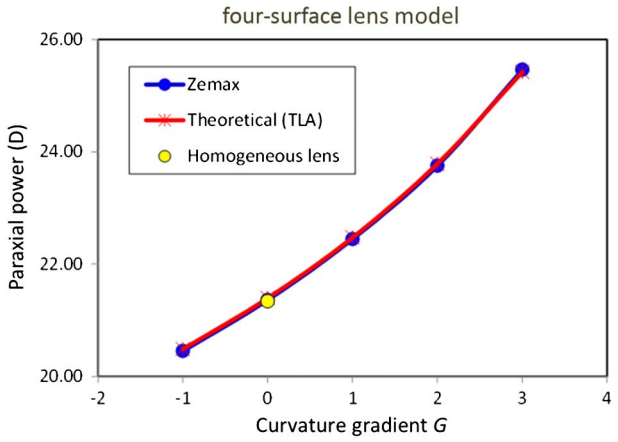

Fig. 2. Paraxial power of a four-surface lens model against the curvature gradient parameter G: Red line and asterisks represent theoretical (thin lens approximation) computation; blue line and circles correspond to Zemax ray tracing. The yellow dot is the power of the homogeneous lens.

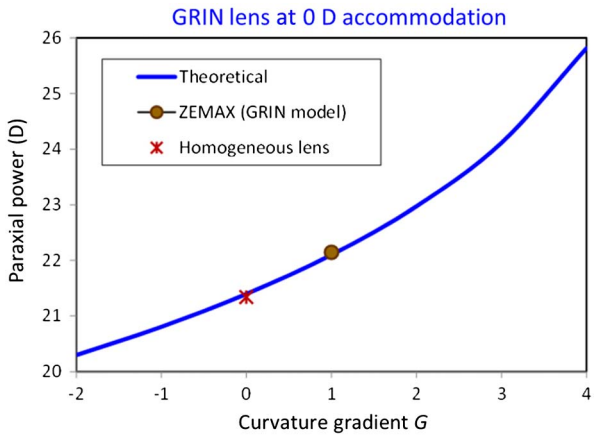

Fig. 3. Paraxial power of the continuous GRIN lens versus the curvature gradient parameter, computed using the thin lens approximation (blue line). Zemax results for the GRIN (brown dot) and homogeneous lens (red asterisk) models are also included.

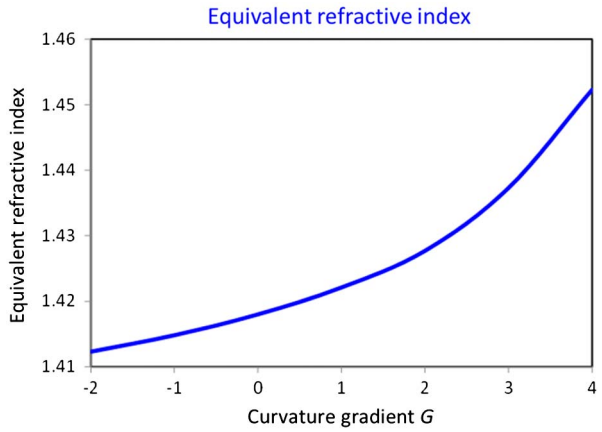

Fig. 4. Equivalent refractive index of the GRIN lens as a function of the curvature gradient parameter.

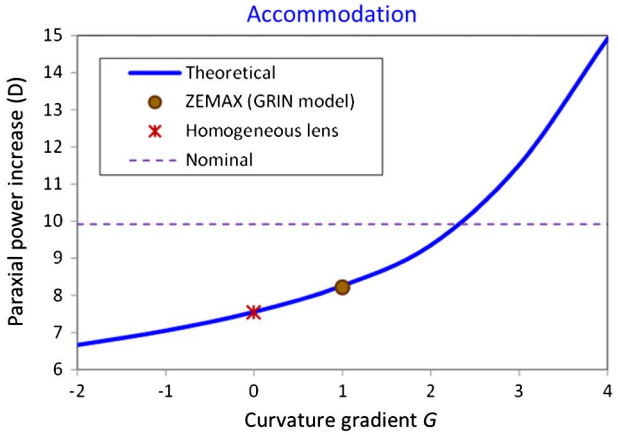

Fig. 5. Increase of lens power due to accommodation as a function of the curvature gradient parameter.

(0 D) and accommodated (8 D nominal accommodation demand) versions of the lens model. The nominal value (9.9 D) is the increase of lens power necessary to obtain an 8 D power increment of the complete eye model. It is straightforward to obtain the relationship between the power increment of the eye caused by an increment of power of the lens:

$$A_{\text{eye}} \simeq (1 - eP_c)A_{\text{lens}}, \tag{9}$$

where P_c is the power of the cornea and e is the distance between the image principal plane of the cornea and the object principal plane of the lens divided by the refractive index of the aqueous humor, n_0. For the Le Grand eye model [26], we have that the increment of power of the lens has to be about 1.24 times higher than that of the eye ($A_{\text{lens}} = 1.24A_{\text{eye}}$). In Fig. 5, the theoretical value reaches the nominal accommodation for $G \approx 2.3$.

5. DISCUSSION AND CONCLUSIONS

We have studied the role of the inner curvature gradient associated with the GRIN distribution on the dioptric power of the lens. There are various assumptions and simplifications involved in this study. Most of them are related to the theoretical analysis, which contains a series of simplifying assumptions, but also to the particular values of the parameters taken from experimental studies. Nevertheless, these values were discussed already [23] and do not essentially affect the main results and conclusions of the present work. A potentially more important simplification is the combination of thin lens and thick lens assumptions used. The thin lens approximation was applied to compute the power of the two (anterior P^{ant} and posterior P^{pos}) parts of the lens. On the one hand, the thick lens formula [Eq. (2)] was then applied to combine these two parts when computing the total power of the lens. Even though this formula is exact in paraxial optics, here we use an effective optical distance corresponding to that of a homogeneous lens with the refractive index of the nucleus. That is, the approximation used in Eq. (2) is exact only for the case $G = 0$. Figure 4 shows that the equivalent refractive index varies with G and hence we can have a slight underestimation (for $G > 0$) or overestimation (for $G < 0$) of the paraxial power. On the other hand, the thin lens approximation was used to obtain Eq. (3), which was used for computing the power of the anterior and posterior parts of the lens. The thin lens approximation tends to overestimate the power because it neglects the negative contribution associated with the optical distance between the refracting surfaces. When $G > 0$, these two errors have opposite signs and partially compensate each other. The numerical results of Fig. 2 show that, for the four-surface shell model, the error is negligible. In the continuous GRIN model, for $G = 1$, the theoretical prediction is slightly lower but the difference is of 0.04 D. The accuracy of the approximation is explained by the fact that most of the gradient is concentrated in the cortex (the nucleus is approximately homogeneous and does not contribute much to the lens power). The thicknesses of the anterior and posterior cortex are of the order of 0.5 mm, and hence they are optically thin to a reasonably good approximation. These results confirm that the accuracy obtained for the computation of the paraxial power by our theoretical approach is high and sufficient for the purposes of this study.

Another potentially interesting issue is the accuracy of the simplified four-surface model to predict the power of the lens. For this purpose, we computed the difference between the theoretical curves of Figs. 2 (four-surface shell model) and 3 (continuous GRIN model) and plotted it in Fig. 6. We can see that there is a substantial difference between these two models, which strongly increases as G departs from 0. The four-surface model

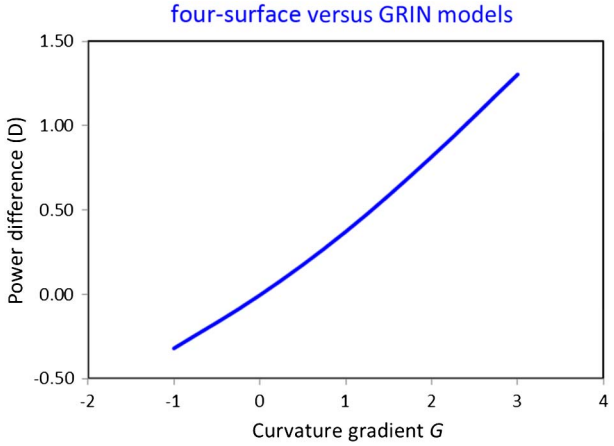

Fig. 6. Difference between the power of the four-surface and GRIN models versus the curvature gradient parameter.

appears to overestimate the effect of G on the lens power as compared to the more realistic GRIN model. The main difference between these two models is that the latter has a smooth change of refractive index, whereas the four-surface model has a sharp discontinuity at the interface between cortex and nucleus. The continuous smooth change in the GRIN lens attenuates the impact of the curvature gradient G on the lens power. Therefore, we conclude that the four-surface model is not realistic enough even to predict the paraxial performance of the lens.

The important role of G may help to explain the lens paradox. Recent experimental evidence suggests a decrease of G with age. In particular, the three panels of Fig. 3 in Ref. [17] show different patterns of the iso-indicial contours. The contours of the young unaccommodated (far-viewing) lens (upper left panel) show some similarity to those of our lens in Fig. 1 for $G = 1$ (concentric case). The young accommodated (near viewing) lens (upper right panel) shows a higher gradient $G > 1$, whereas the older lens (lower panel) shows a clear negative $G < 1$ curvature gradient. Experimental evidence supports a progressive gradual decrease of lens power with aging. A recent study [2] suggests that this decrease is of the order of 3 D. In Fig. 6, a change from $G = 2$ to $G = -1$ may explain a decrease of 3.3 D. Thus an age-related decrease of G by about 3 could explain the observed decline in lens power. Nevertheless this is assuming constant geometry, which is not the case since external lens curvatures increase with age [13]. Thus, we believe that any effective explanation of the lens paradox should take into account the contribution of the (plausible) decrease of G with age. Nevertheless, more experimental data are needed to assess the age-related changes of G.

Figure 5 shows that G also enhances accommodation. These results were obtained assuming that G is constant and does not change with accommodation. We assumed the simplest case, but Fig. 3 in Ref. [17] (cited in the previous paragraph) suggests an increase of G when comparing the lens for far and near viewing. An accommodation-related increase of G would produce an additional enhancement of the accommodation response. Nevertheless, *in vivo* experimental data on the changes of the GRIN lens upon accommodation are still too scarce to get a solid conclusion. This effect will explain the intracapsular mechanism of accommodation (ICMA) postulated by Gullstrand [27–29] to explain the fact that the increment of external curvature of the lens alone does not explain the increase of power necessary to accommodate. The ICMA means that the equivalent refractive index should increase with accommodation as well. Our results, obtained for the simplest case when G does not change with accommodation, indicate that a positive ICMA (increase of n_{eq}) is obtained only when the curvature gradient is positive ($G > 0$). For instance, when $G = 2$, the equivalent refractive index (n_{eq}) of our GRIN model increases by 0.0036 from 0 to 8 D of accommodation. Of course, that increase would be higher in the case in which G also increases with accommodation. In its theoretical eye model, Le Grand assumed a roughly double increase of 0.007 (from 1.420 to 1.427 when passing from 0 to 7.7 D of accommodation) [26]. We estimate that such increase of n_{eq} would correspond to an increase of G with accommodation by about 1.5. Gullstrand hypothesized an even higher ICMA, with an increase of around 0.0175 of n_{eq} for its four-surface model. We estimated that such a huge ICMA is associated with a curvature gradient of about 3.8 for the anterior lens, which seems too high compared to more recent data on curvature of the lens cortex and nucleus [20].

Our main theoretical result, $P = P_{HOM} + Gp_{GRIN}$, is that the power has two contributions: one is the power of a lens with homogenous refractive index n_n, which is totally independent from the type of gradient; the other is given by the gradient, which is a combination (product) of the contributions of both curvature and index gradients. A similar rule can be applied to accommodation. As an example, we can consider the values of Fig. 5 for $G = 2$. We find that the increase of lens power is 9.35 D whereas the contribution of P_{HOM} is 7.56 D, that is, the GRIN only contributes 19.1% of the total accommodation, whereas P_{HOM} contributes 80.9%. This contrasts with other studies. Maceo *et al.* [30] estimated a much higher contribution of the GRIN of about 65% in monkeys and baboons, compared to less than 20% in our estimations. This large discrepancy can be explained by their definition of the GRIN contribution. For the homogeneous lens, they assume the refractive index at the surface n_s instead of n_n (nucleus), which is the parameter that naturally appears in our formulation. If we consider n_s instead of n_n, the homogeneous lens power decreases drastically from 21.4 D to only 9.14 D, so the apparent effect of the GRIN becomes much higher. In terms of accommodation, for $G = 2$, the contribution of P_{HOM} will decrease from 7.56 D to only 4.86 D (52%). With this definition of P_{HOM}, the contribution of the GRIN will be almost 50%, which is substantially closer to the values found in primates (65%) even considering that these percentages correspond to different species. Nevertheless, using the surface index n_s to estimate the contribution P_{HOM} does not seem supported by the theory.

The main conclusion of the present work is that the curvature gradient is a key factor in the refractive index distribution of the lens, as appears explicitly in the expression $P = P_{HOM} + Gp_{GRIN} = P_{HOM} + P_{GRIN}$. Strictly speaking, it only applies to the anterior and posterior parts of the lens separately whereas, for computing the total power of the lens, one must also take into account the cross terms [Eq. (7)]. It appears to provide a fine tuning of the lens power with a real impact of changing the power of the crystalline lens, and hence we believe that realistic GRIN lens models should explicitly or implicitly [22] consider the inner curvature gradient. A positive curvature gradient (which seems to be the case in young human lenses [21]) provides an effective increase to the lens power and vice versa. This is relevant in aging and accommodation of the lens: On the one hand, an age-related decrease of the curvature gradient [21] may be a key factor in explaining the lens paradox; on the other hand, the curvature gradient may significantly enhance the increase of lens power during accommodation. In fact, the increase of the effective refractive (intracapsular mechanism) appears to mainly depend on G.

Funding. H2020 European Research Council (ERC) (ERC-2012-StG 309416-SACCO).

REFERENCES

1. R. Navarro, "Adaptive model of the aging emmetropic eye and its changes with accommodation," J. Vis. **14**(13), 21 1–17 (2014).
2. S. Jongenelen, J. J. Rozema, and M.-J. Tassignon, EVICR.net, and Project Gullstrand Study Group, "Distribution of the crystalline lens power

in vivo as a function of age," Invest. Ophthalmol. Vis. Sci. **56**, 7029–7035 (2015).
3. B. K. Pierscionek, "Refractive index contours in the human lens," Exp. Eye Res. **64**, 887–893 (1997).
4. C. Jones, D. Atchison, R. Meder, and J. Pope, "Refractive index distribution and optical properties of the isolated human lens measured using magnetic resonance imaging (MRI)," Vision Res. **45**, 2352–2366 (2005).
5. A. de Castro, S. Ortiz, E. Gambra, D. Siedlecki, and S. Marcos, "Three-dimensional reconstruction of the crystalline lens gradient index distribution from OCT imaging," Opt. Express **18**, 21905–21917 (2010).
6. B. Pierscionek, M. Bahrami, M. Hoshino, K. Uesugi, J. Regini, and N. Yagi, "The eye lens: age-related trends and individual variations in refractive index and shape parameters," Oncotarget **6**, 1–13 (2015).
7. A. Glasser and M. C. Campbell, "Presbyopia and the optical changes in the human crystalline lens with age," Vision Res. **38**, 209–229 (1998).
8. A. Roorda and A. Glasser, "Wave aberrations of the isolated crystalline lens," J. Vis. **4**, 250–261 (2004).
9. G. Smith, D. A. Atchison, and B. K. Pierscionek, "Modeling the power of the aging human eye," J. Opt. Soc. Am. A **9**, 2111–2117 (1992).
10. R. Navarro, F. Palos, and L. González, "Adaptive model of the gradient index of the human lens. I. Formulation and model of aging *ex vivo* lenses," J. Opt. Soc. Am. A **24**, 2175–2185 (2007).
11. J. A. Díaz, C. Pizarro, and J. Arasa, "Single dispersive gradient-index profile for the aging human lens," J. Opt. Soc. Am. A **25**, 250–261 (2008).
12. M. Bahrami and A. V. Goncharov, "Geometry-invariant gradient refractive index lens: analytical ray tracing," J. Biomed. Opt. **17**, 055001 (2012).
13. N. P. Brown, "The change in lens curvature with age," Exp. Eye Res. **19**, 175–183 (1974).
14. J. F. Koretz and G. H. Handelman, "How the human eye focuses," Sci. Am. **259**, 92–99. (1988).
15. B. K. Pierscionek, "Presbyopia-effect of refractive index," Clin. Exp. Optom. **73**, 23–30. (1990).
16. N. P. Brown, J. F. Koretz, and A. J. Bron, "The development and maintenance of emmetropia," Eye **13**, 83–92 (1999).
17. M. Dubbelman and G. L. Van der Heijde, "The shape of the aging human lens: curvature, equivalent refractive index and the lens paradox," Vision Res. **41**, 1867–1877 (2001).
18. B. A. Moffat, D. A. Atchison, and J. M. Pope, "Explanation of the lens paradox," Optom. Vis. Sci. **79**, 148–150 (2002).
19. R. Navarro, J. Santamaría, and J. Bescós, "Accommodation-dependent model of the human eye with aspherics," J. Opt. Soc. Am. A **2**, 1273–1281 (1985).
20. E. A. Hermans, M. Dubbelman, R. Van der Heijde, and R. M. Heethaar, "Equivalent refractive index of the human lens upon accommodative response," Optom. Vis. Sci. **85**, 1179–1184 (2008).
21. S. Kasthurirangan, E. L. Markwell, D. A. Atchison, and J. M. Pope, "*In vivo* study of changes in refractive index distribution in the human crystalline lens with age and accommodation," Invest. Ophthalmol. Visual Sci. **49**, 2531–2540 (2008).
22. C. Sheil and A. Goncharov, "Accommodating volume-constant age-dependent optical (AVOCADO) model of the crystalline GRIN lens," Biomed. Opt. Express **7**, 1985–1999 (2016).
23. R. Navarro, F. Palos, and L. González, "Adaptive model of the gradient index of the human lens, II: optics of the accommodating aging lens," J. Opt. Soc. Am. A **24**, 2911–2920 (2007).
24. E. A. Hermans, M. Dubbelman, R. Van der Heijde, and R. M. Heethaar, "The shape of the human lens nucleus with accommodation," J. Vis. **7** (10), 1–10 16 (2007).
25. W. N. Charman and D. A. Atchison, "Age-dependence of the average and equivalent refractive indices of the crystalline lens," Biomed. Opt. Express **5**, 31–39 (2014).
26. Y. Le Grand and S. G. El Hage, *Physiological Optics* (Springer-Verlag, 1980).
27. A. Gullstand, "How I found the mechanism of intracapsular accommodation," Nobel Lecture (Dec. 11, 1911).
28. A. Gullstand, "Mechanism of accommodation," in *Handbuch der Physiologischen Optic*, H. Helmholtz von, ed. (1909), Appendix IV, pp. 383–415.
29. J. P. C. Southall, *Trans.: Helmholtz's Treatise on Physiological Optics* (Dover, 1962).
30. B. M. Maceo, F. Manns, D. Borja, D. Nankivil, S. Uhlhorn, E. Arrieta, A. Ho, R. C. Augusteyn, and J. M. Parel, "Contribution of the crystalline lens gradient refractive index to the accommodation amplitude in non-human primates: *in vitro* studies," J. Vis. **11**(13), 23 1–13 (2011).